Science of the Total Environment 865 (2023) 161255

Contents lists available at ScienceDirect

Science of the Total Environment

journal homepage: www.elsevier.com/locate/scitotenv

Exploration of occurrence and sources of microplastics (>10 μm) in Danish marine waters

Yuanli Liu [a,*], Claudia Lorenz [a], Alvise Vianello [a], Kristian Syberg [b], Asbjørn Haaning Nielsen [a], Torkel Gissel Nielsen [c], Jes Vollertsen [a]

[a] Department of the Built Environment, Aalborg University, Thomas Manns Vej 23, 9220 Aalborg, Denmark
[b] Department of Science and Environment, Roskilde University, Universitetsvej 1, DK-4000 Roskilde, Denmark
[c] National Institute of Aquatic Resources, Technical University of Denmark, Kemitorvet, Building 202, DK-2800 Kgs. Lyngby, Denmark

HIGHLIGHTS

- MP number and mass concentrations tell a different story.
- Fragments of polyester, PP, and PE dominated.
- The carbonyl indices increased with decreased sizes.
- Wastewater and stormwater contribute a significant fraction to the marine MPs.

GRAPHICAL ABSTRACT

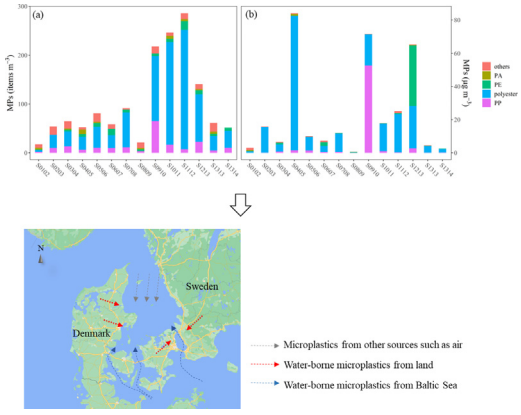

ARTICLE INFO

Editor: Dimitra A Lambropoulou

Keywords:
Microplastics
MP abundance
Mass concentration
μFTIR-imaging
Microplastic sources

ABSTRACT

Microplastics (MPs) were quantified in Danish marine waters of the Kattegat and the southernmost part of Skagerrak bordering to it. Kattegat is a waterbody between Denmark and Sweden that receives inflow from the Baltic Sea and direct urban runoff from the metropolitan area of Copenhagen and Malmö. MPs were measured in 14 continuous transects while steaming between monitoring stations. MP levels tended to be highest close to the Copenhagen-Malmö area, albeit this was more obvious from the abundance of particles rather than mass. The outcome of the measurements allowed a rough MP budget in the Danish Straits region, suggesting that urban waste- and stormwater discharges could not be neglected as potential MP source in these waters. The marine samples were collected by pumping and filtering water over 10 μm steel filters, hereby sampling a total of 19.3 m^3. They were prepared and analyzed by FPA-μFTIR imaging, and the scans interpreted to yield MP size, shape, polymer type, and estimated mass. The average concentration was 103 ± 86 items m^{-3}, corresponding to 23.3 ± 28.3 μg m^{-3} (17–286 items m^{-3}; 0.6–84.1 μg m^{-3}). Most MPs were smaller than 100 μm and fragments dominated the samples. The carbonyl index was assessed for polyolefins, showing that oxidation increased with decreasing MP size, but did not correlate with distance to urban areas. A rough budget of MP in the Danish Straits region suggested that MPs discharged from urban waste- and stormwaters were an import source of MPs.

* Corresponding author.
E-mail address: yuanlil@build.aau.dk (Y. Liu).

http://dx.doi.org/10.1016/j.scitotenv.2022.161255
Received 29 September 2022; Received in revised form 16 December 2022; Accepted 24 December 2022
Available online 31 December 2022

1. Introduction

Microplastics (MPs) have received much attention over the last decades (Frias and Nash, 2019; Mathalon and Hill, 2014). They are intentionally produced for commercial purposes, such as in cosmetics (Wright et al., 2013), or derived from the fragmentation of larger plastic items (Jaikumar et al., 2019). These small MPs are bioavailable and potentially pose a threat to the ecosystem and human-beings through the food chain or directly from the air (Akhbarizadeh et al., 2020a; Akhbarizadeh et al., 2020b; Akhbarizadeh et al., 2021; Cunha et al., 2020; Kashfi et al., 2022).

Many studies have attempted to quantify MPs in the marine environment (Everaert et al., 2020; Jiang et al., 2020a; Jiang et al., 2020b). However, even within the same waterbody, there are large differences in reported concentrations; for example, in the Northwest Pacific where reported concentrations vary several orders of magnitude even when comparable sampling methods were applied (Mu et al., 2019; Pan et al., 2019a, 2019b). Some of the differences can be explained by the patchiness of MPs, while other probably are due to variations in the applied gear, sample preparation (Dai et al., 2018; Zhang et al., 2017) and analytical methods (Teng et al., 2020; Zhao et al., 2015). Furthermore, most studies focused on stationary sampling (Buckingham et al., 2022; Liu et al., 2021), which may be more prone to local patchiness than continuous sampling along transects. Nevertheless, these differences in reported values for the same area indicate that there are true concentration differences in the sea due to heterogenic distribution, especially for areas with relatively low concentrations of plastic particles (Buckingham et al., 2022; Liu et al., 2021).

Most studies have quantified MPs larger than 300 μm because sampling was conducted with a net or manta trawl (Bakir et al., 2020; Eo et al., 2019; Ferreira et al., 2020; Syberg et al., 2017). Mesh size matters for how much MP is found, and different sizes can lead to significant differences in reported concentrations (Lindeque et al., 2020). Furthermore, less specialized analytical equipment has commonly been used to detect microplastics, for example, manual sorting and counting using stereo microscopy (Renner et al., 2018). Even when combined with chemical identification of selected particles, this leads to increased uncertainties when attempting to quantify small MPs as these are difficult to sort out from a sample. This has led to limited knowledge of MPs below roughly 200 μm (Simon-Sánchez et al., 2022a). Over the past decade, all parts of the MP quantification approach have developed significantly. With respect to sampling, pumped filtration was introduced to efficiently collect MPs by filtering on-site down to 10–20 μm (Enders et al., 2015; Rist et al., 2020). Sample preparation protocols have been refined (Löder et al., 2017; Lorenz et al., 2019), and chemical analysis has substituted visual identification by stereo microscopy to reduce analytical bias (Sridhar et al., 2022). Analytical techniques for quantifying ever-smaller MPs have furthermore been developed and refined, e.g., imaging with Focal Plane Array (FPA)-Fourier Transform Infrared Spectroscopy (FTIR) and Raman spectroscopy as well as Pyrolysis Gas Chromatography-Mass Spectrometry (Py-GC–MS) (Ye et al., 2022).

It is well-known that marine plastic debris is mainly sourced from land, where almost 80 % of the marine plastic debris originates (Li et al., 2016). Land-based plastics are commonly believed to be mainly transported by rivers and wastewater treatment plant effluent into the marine environment (Fendall and Sewell, 2009; Geyer et al., 2017; Li et al., 2016). Wastewater is a significant pathway for MPs into the environment because of its high MP content (Rasmussen et al., 2021; Sundt et al., 2014), even when treated by advanced facilities (Estahbanati and Fahrenfeld, 2016; Mahon et al., 2017). Wastewater is furthermore discharged untreated by combined sewer overflows and sewage misconnected to storm drains. Additionally, cities, rural roads and highways generate separate stormwater, which also contains significant amounts of MP (Liu et al., 2019a, 2019b). In addition to the water-borne MPs, the marine environment receives MPs from marine sources, e.g., breakdown of fishing nets, as well as an unknown amount of air-borne MPs. The latter has, for example, been documented in snow from remote areas like the Arctic, Antarctica, and the Swizz alps (Aves et al., 2022; Bergmann et al., 2019).

Once MPs enter the environment, they will undergo weathering governed by environmental conditions such as oxygen levels, light, temperature, and biofilm coverage (Mei et al., 2020; Turgay et al., 2019; Wang et al., 2020a, 2020b). In general, marine water has a lower temperature than land and will also partly protect the MPs against sunlight. Their weathering rate in the aquatic environment can hence be assumed to be slower than on a terrestrial surface (Duan et al., 2021). One could hypothesize that MPs are increasingly weathered the longer they have been in the environment and that weathering indexes potentially can be used to identify closeness to sources, though this is still rather speculative.

Kattegat receives brackish water from the Baltic Sea via three straits, which mixes with saline waters from the Skagerrak. Despite advances in the field of MP research, knowledge of their abundance and distribution in these waters is still scarce (Bagaev et al., 2018; Beer et al., 2018; Gewert et al., 2017; Schönlau et al., 2020; Setälä et al., 2016; Tamminga et al., 2018; Zhou et al., 2021). Hence, the aim of this study is to investigate the abundance, distribution, and composition of MPs in the Kattegat down to 10 μm and assess whether there is a relationship between abundance and proximity to major urban sources.

2. Materials and method

2.1. Study area

The study area is the Kattegat (Fig. 1), covering 30,000 km^2 and the southernmost part of Skagerrak bordering up hereto. Kattegat borders the Baltic Sea by the Danish Straits to the south and is surrounded by Denmark to the south and the west and Sweden to the east. Its waters are mostly stratified, with the lower layer consisting of inflowing seawater from the North Sea via Skagerrak (Gröger et al., 2019). The upper layer consists of inflowing brackish Baltic Sea water. These two opposing flows transport a net surplus of 475 km^3 from the Baltic to the Skagerrak annually. During stronger winds, the layers in the Kattegat are thoroughly mixed in areas such as the Great Belt, so the overall salinity is highly variable in this semi-enclosed basin (Physical Oceanography of the Baltic Sea, n.d.).

2.2. Sampling

Sampling was conducted from 24th to 30th of October 2020 onboard the R/V Dana (DTU Aqua). The samples were collected using the Universal Filtering Object (UFO), a pump-filter device developed by Aalborg University to sample marine waters down to 10 μm (Rist et al., 2020). The UFO system was composed of three interconnected and closed steel filter holders containing one 300 μm and two 10 μm stainless steel filters (Ø = 167 mm), respectively. The average flowrate was 7 L min^{-1}. The water is pre-filtered by the 300 μm filter, then the water flow split, and the water is filtered further onto the two parallel-coupled 10 μm filters. The outflow is recombined and measured by a mechanical flowmeter. The filtering device was connected to the saltwater ship intake and placed in the ship's wet lab. The inlet of the intake is located 3 m below the waterline on the forward port side. Transect samples were collected between 14 stations during steaming (Fig. 1), and filters were changed approx. Every 3 h or when they clogged. Depending on the distance between stations, some transect samples consisted of more than one filter set. In total, 20 filter sets were collected, and stored in glass Petri dishes at 4 °C in the dark before analysis. The 300 μm and 10 μm filters of each UFO-sample were pooled into one set and all sets processed individually. If a transect consisted of more than one set, the results of the individual sets were pooled into one result per transect. Each result was named by its transect. For example, the sample collected between stations 1 and 2 was named S0102. One sample, named S1313, covered a rather short distance from 57.52°N, 10.54°E to 57.54°N, 10.51°E (Table 1), as shown in the Fig. 1.

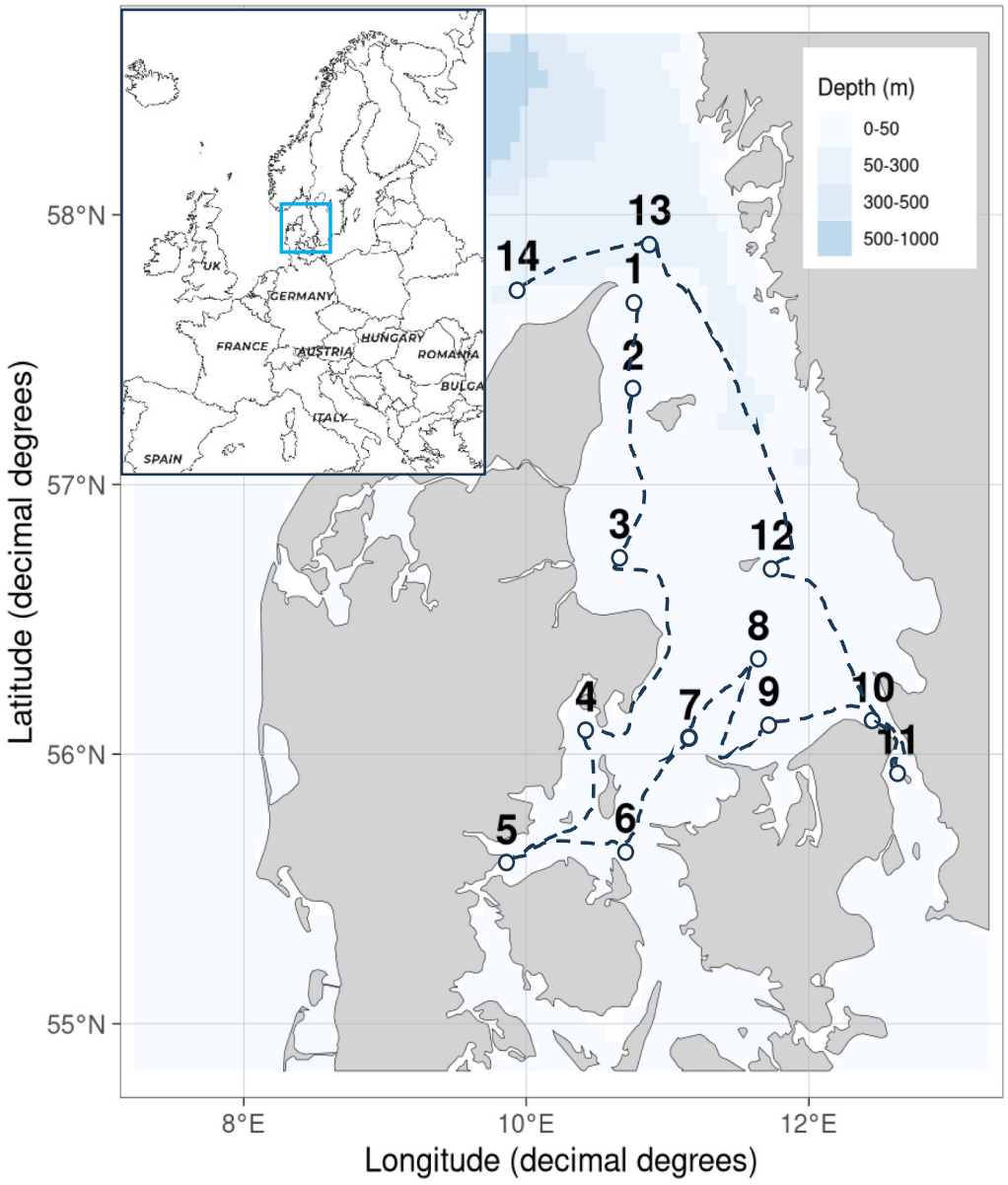

Fig. 1. Transect sampling map. The site numbers indicate the begin and end of a sampling transect. The dash lines between site numbers show the sailing route during sampling.

2.3. Sample preparation

The samples were processed following a multistep enzymatic-oxidative protocol to extract MPs from the matrix (Liu et al., 2019a, 2019b; Rist et al., 2020; et al., 2018). In short, the filters were first incubated in 5 % sodium dodecyl sulphate (SDS) solution to help get all material off the filter. Then protease (Sigma, Protease from Bacillus sp.), cellulase (Sigma, Cellulase enzyme blend), and Viscozyme® L (Sigma) were applied consecutively to digest natural proteins and cellulose, respectively. Following that, a Fenton oxidation was done to remove the remaining organic matter. A density separation with SPT (Sodium Polytungstate) solution (1.70–1.80 g cm^{-3}) was used to separate lighter particles from inorganic ones. After washing the extracted particles carefully, the sample was evaporated and stored in 10 mL vials. 5 mL of 50 % ethanol (EtOH) was added to each vial to ensure a known extract volume. Between steps, particles were collected on 10 μm steel filters (Ø = 47 mm). And the same filters was used throughout the whole sample extraction to minimize loss of particles.

2.4. MP identification

Extracts stored in 5 mL EtOH were homogenized on a vortex mixer, and subsamples were taken with a glass pipette in 50/100 μL increments. These were deposited on a Ø 13 × 2 mm zinc selenide window (Crystran, UK), held in a compression cell (Pike Technologies, USA) with a 10 mm diameter free area and dried at 50 °C. After every deposition, the window was checked under a microscope until it was sufficiently populated and ready for scanning. Three windows were deposited per sample, achieving a scanning of 16–50 % of the total sample and blanks. All scan results were then scaled back to the full sample, i.e., the 5 mL of EtOH. The scan was done with an Agilent Cary 620 FTIR microscope equipped with a 128 × 128 pixels FPA (Focal Plane Array, Mercury Cadmium Telluride detector) coupled with an Agilent 670 IR spectrometer. The microscope was equipped with a 15× Cassegrain objective, yielding a 5.5 μm pixel resolution. All scans were performed in transmission mode with a spectral range of 3750–850 cm^{-1} at 8 cm^{-1} resolution applying 30 co-added scans. The background was created by co-adding 120 scans.

Table 1
Locations of start of transects, sampling time, sampled volume, and wind direction.

Station Code	N	E	Wind Direction	Total time	Sampled Volume (m^3)	Transects
S0102IWD24T03	57.42	10.48	SW 220° 10.2 m/s	03:20	1.157	S0102
S0203IWD24T12-1	57.21	10.43	S 190° 11.2 m/s	04:53	1.219	S0203
S0203IWD24T12-2				02:22	0.601	S0203
S0304IWD24T23-1	56.41	10.37	S 170° 9.8 m/s	03:06	1.044	S0304
S0304IWD24T23-2	56.23	11.01	S 180° 15.5 m/s	03:57	1.092	S0304
S0405IWD25T-1	56.05	10.25	SW 205° 11.6 m/s	02:31	0.993	S0405
S0405IWD25T-2	55.41	10.19	SW 195° 10.2 m/s	01:55	0.775	S0405
S0506IWD26T00	55.36	09.51	S 190° 6.5 m/s	03:19	1.101	S0506
S0607IWD26T11	55.39	10.42	S 180° 7.8 m/s	02:58	0.857	S0607
S0708IWD26T20	56.04	11.09	SW 215° 9.7 m/s	02:38	0.977	S0708
S0809IWD27T03	56.20	11.36	S 190° 11.2 m/s	04:53	1.219	S0809
S0910IWD27T15	56.07	11.44	S 190° 10.2 m/s	03:16	0.984	S0910
S1011IWD28T01	56.07	12.27	S 180° 9.2 m/s	02:16	0.903	S1011
S1112IWD28T-1	55.56	12.38	SW 225° 10.5 m/s	03:09	1.012	S1112
S1112IWD28T-2	56.22	12.16	SW 210° 12.6 m/s	02:56	0.793	S1112
S1213IWD28T23-1	56.41	11.41	SW 205° 9.5 m/s	03:06	0.900	S1213
S1213IWD28T23-2	57.14	11.37	SW 210° 13 m/s	02:12	0.780	S1213
S1213IWD28T23-3	57.38	11.14	SW 210° 10 m/s	02:03	0.790	S1213
S1313IWD29T17	57.52	10.54	SW 270° 5.2 m/s	01:47	0.803	S1313
S1314IWD30T01	57.54	10.51	SW 225° 5.8 m/s	03:30	1.344	S1314

2.5. Data analysis

The spectral data from the μFTIR imaging were analyzed by siMPle, a software developed for automatic MP identification (Primpke et al., 2020), applying the detection algorithm described in Liu et al. (2019a, 2019b). The library was based on the one used by Rist et al. (2020) but extended to 475 reference spectra. It covered 74 material types, including plastics, organic and inorganic matter (Supplementary Information (SI) Table S1). Baseline correction was applied to all sample spectra before analysis (Primpke et al., 2018). A particle was identified as MP if it took up at least 2 pixels, yielding a minimum detection size of 11 μm. A carbonyl index was calculated for the polyolefins polyethylene (PE) and polypropylene (PP) from the ratio between the integrated band absorbance of the carbonyl (C═O) peak from 1850 to 1650 cm^{-1} and that of the methylene (CH_2) scissoring peak from 1500 to 1420 cm^{-1} to indicate the oxidation state (Almond et al., 2020; Simon-Sánchez et al., 2022b). An index was calculated for each spectrum (pixel) of an MP, and the overall index was taken as the average of all individual indexes. siMPle provided the information on the size (minor and major dimensions), polymer type, and mass, where the latter was estimated based on the volume of the particle assuming an ellipsoid shape and the density of its material (Rist et al., 2020; Simon et al., 2018). Fibers were defined as MPs whose length-to-width ratio was large than 3 (Cole, 2016; Vianello et al., 2019).

After the analysis, the spectra of all identified MPs were checked manually to remove false-positive particles. To make siMPle perform better, representative spectra of false-positive particles were added to the library (Fig. S1), and the threshold of different polymers was adjusted based on the result. Detailed information on the library is shown in Table S1, and the information for some spectra is exemplified in Fig. S1. After the analysis, all data were visualized in R (v4.0.3). Principle component analysis (PCA) was carried out to estimate variables that explained most of the variations.

2.6. Contamination control

Several measures were taken to avoid contamination with synthetic fibers and particles. Cotton lab coats were worn during the sample preparation. The air in the FTIR and microscope room was continuously filtered with a Dustbox® (Hochleistungsluftreininger, Möcklinghoff Lufttechnik, Germany) housed with a HEPA filter (H14, 7.5 m^2). All sample preparation was performed inside a Scan-Laf Fortuna Clean Bench (Labogene, Denmark), which was cleaned with 50 % EtOH before use. All glassware and stainless-steel filters were muffled at 500 °C before use, and all other equipment was rinsed three times with Milli-Q water during the whole process. Reagents were prepared, filtered through 0.7 μm muffled glass fiber filters, and stored in muffled glassware.

Despite all taken measures, it is impossible to completely avoid contamination with MPs. To account for this, ship blanks and procedural lab blanks were collected. Three ship blanks were collected during the sampling on the ship by opening a muffled glass petri dish every time the UFO sampling device was opened to account for potential air-borne contamination. As shown in Table 2, the three ship blanks corresponded to a total of 35 filter sets, of which 20 were used in this study and the remaining 15 used to collect stationary samples during the same cruise. The contamination in the ship blank per set of filters was calculated as 1/35th of the total MP content found in the three ship blanks. The five procedural lab blanks followed the sample preparation of the real samples but with Milli-Q water as the matrix. Like what was done for the marine samples, subsamples of 16 % – 50 % were taken of the blanks, scanned, and calculated to the 5 mL of the full sample. A blank correction was done based on both the ship blanks and the lab blanks and per polymer type (Mani et al., 2019; Rist et al., 2020). The ship blanks per filter set and the median of the lab blanks were calculated and subtracted from the result of each set of UFO filters. Where a transect consisted of more than one filter set, the results were merged after blank subtraction from each set.

2.7. Quality control and recovery test

To quantify MPs in samples, it is necessary to calculate the limit of detection (LOD) and limit of quantification (LOQ). The applied equations were:

$$LOD = X_{blank} + 3.3^{*} S_{blank} \quad (1)$$

$$LOQ = X_{blank} + 10^{*} S_{blank} \quad (2)$$

where S_{blank} is the standard deviation of the blanks and X_{blank} is their mean. The approach of using 3.3 and 10 times the standard deviation on the blanks is recommended by the Association of Official Agricultural Chemists (AOAC International) (Horton et al., 2021), while the approach of adding the mean of the blanks is recommended by Armbruster and Pry (2008).

Recovery experiments were conducted to assess the losses of microplastics during sample processing. A triplicate of standard plastic microspheres was created by mixing 150 PE microspheres (90–106 μm) of three different densities (0.98 g cm^{-3}: fluorescent blue-green, 1.13 g

Table 2
MPs per blank sample after calculation, ship and procedural lab blanks.

Group	Acrylates	polyester	PAN_acrylic fiber	PA	ABS	PP	PE	polysulfone	EVA	Total
Ship blank 1	6.3	43.8	0	0	0	0	0	0	0	50.1
Ship blank 2	0	28.1	0	9.4	0	3.1	0	0	0	40.1
Ship blank 3	0	12.5	0	0	0	0	6.3	0	0	18.8
Lab blank 1	0	2.8	0	0	0	0	0	0	0	2.8
Lab blank 2	0	6.5	0	0	0	0	0	0	0	6.5
Lab blank 3	0	0	0	0	0	0	0	0	0	0
Lab blank 4	0	138	0	0	2.1	4.2	6.3	2.1	2.1	156.9
Lab blank 5	0	25	4.2	2.1	0	0	2.1	0	0	33.4

cm^{-3}: fluorescent blue, and 1.20 g cm^{-3}: fluorescent red; Cospheric LLC), 50 of each type. The spheres were spiked into 5 % SDS solution in a crystallization dish and processed following the previously described sample preparation process. The number of PE spheres in the final extract was counted under an optical microscope (Dino-Lite Edge AM4115TL, 10-140× magnification) illuminated with UV light (OP UV LED, 365 nm).

The recovery rate was calculated as follows:

$$R = N_2/N_1 \quad (3)$$

where N_1 and N_2 refer to number of spheres before and after sample preparation, respectively.

3. Results

3.1. Blanks and recovery test

The ship blanks covering 35 individual sets of UFO samples contained a total of 109 MPs, most of which were polyester while some were acrylates, polyamide (PA), polypropylene (PP) and polyethylene (PE) (Table 2). The contamination per sample was hence on average 1/35 × 109 = 3.11 MPs. The lab blank 4 (Table 2) related to sample S0809 held a much higher MP count because the sample S0809 (the transect between stations 8 and 9) unexpectedly had to be cooled down by adding ice during the Fenton reaction. The ice was not particle-free and to assess the contamination, the same amount of ice was added to lab blank 4, and sample S0809 was corrected by this value (Table S2). Of the lab blanks, no. 5 showed substantially higher values than the others. Compared to the 'ship blank per sample', i.e., the 3.11 MPs per sample, it was 10 times higher than the others. The reason here is unknown but indicates that such occasional high contamination can also occur for real samples. The high value furthermore means that the blank values were not normal distributed and the basic assumption behind Eqs. (1) and (2) hence not met. To calculate LOD and LOQ, it was chosen to omit this value, yielding LOD and LOQ values of 9.8 and 23.5 MPs per sample, respectively, for the total number of particles found. Even though the LOD and LOQ differ between polymer types, it was chosen only to calculate these values for the total number of MPs as the numbers in the blanks were too small to yield meaningful LOD and LOQ values per polymer type. Blank correction, on the other hand, was done polymer by polymer. Where this led to negative values in the samples (i.e., there were more MPs of a certain polymer type in the blank sample than in the marine sample), these were set to zero.

The recovery test yielded 90.3 % ±1.1 % recovery (Table S3) with no significant difference for the various densities. While this recovery is deemed quite good, it must be kept in mind that it only covered a selection of particle sizes, shapes, polymer types, and densities. It cannot be excluded that recovery for other MPs differed from the ones found for the microspheres.

3.2. MP abundance

A total of 20 filter sets were collected and pooled into 14 transects (Fig. 2). The blank-corrected abundance measured as particle counts ranged from 17 to 286 items m^{-3}, with an average concentration of

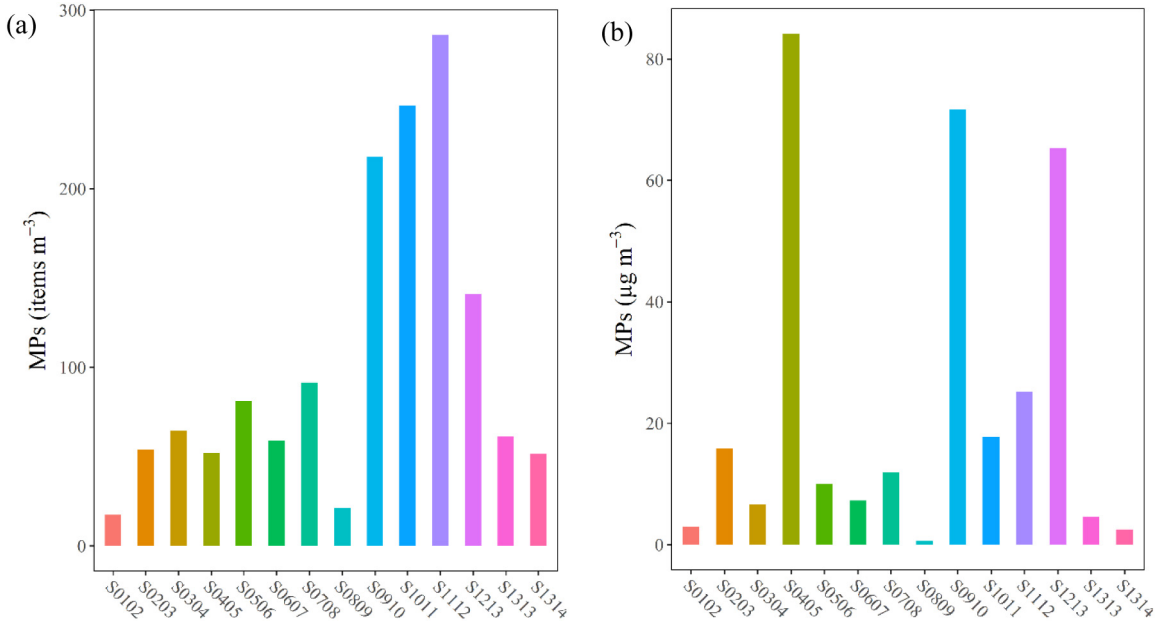

Fig. 2. Total (a) MP abundance per transect (b). MP mass concentration per transect estimated from the μFTIR analysis.

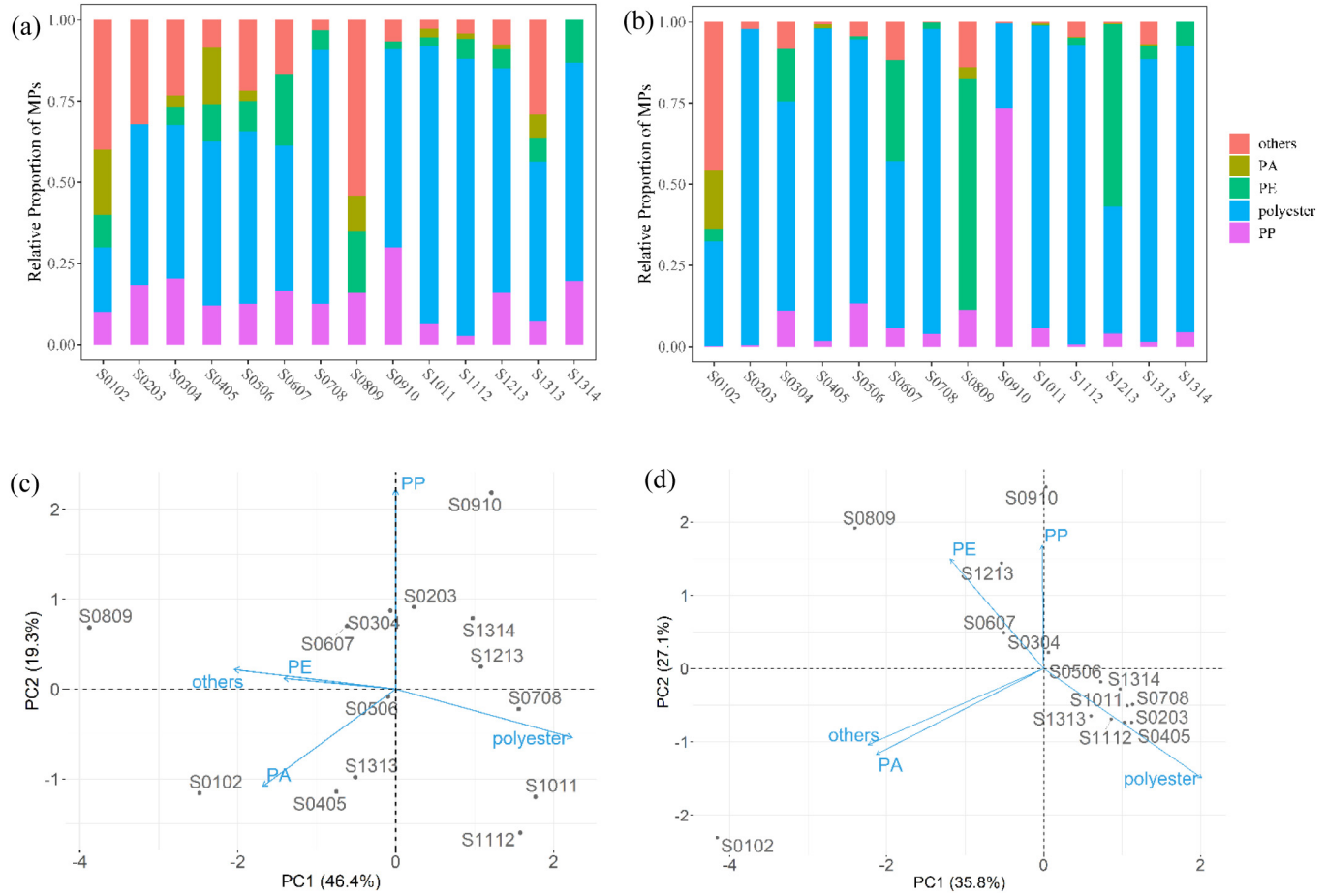

Fig. 3. Relative proportion of (a) MP abundance (items m^{-3}), (b) Estimated MP mass concentrations (μg m^{-3}). Principal components analysis for (c) MP abundance, (d) Estimated MP mass concentrations.

103 ± 86 items m^{-3} (Fig. 2a). In other words, all values were above the calculated LOD but not all were above the LOQ. The highest counts were in the transects from stations 9 to 12, while counts between stations 1 to 9 and 13 to 14 were below average. The highest concentration was found in the transects north of the Copenhagen area (S1112).

The MP mass concentrations ranged from 0.6 to 84.1 μg m^{-3} with an average of 23.3 ± 28.3 μg m^{-3} (Fig. 2b). The mass concentrations were distributed differently compared to the counts (Fig. 2a). Transect S0405 had the highest concentration, followed by transect S0910 and S1213. Nevertheless, the transects 1 to 4, 5 to 9, and 13 to 14 had comparatively low concentrations for both mass and numbers.

3.3. MP composition

The MPs identified belonged to 21 polymer groups, of which 17 accounted for <1 % each in terms of MP numbers. These were pooled into one group termed “others” (Table S1). The 4 groups which each contributed >1 % of the total were polyester, PA, PE, and PP (Fig. 3). Polyester was the largest group both in terms of counts and mass, followed by PP and “others”. When it came to spatial distribution, the composition of MPs varied between transects. A PCA was conducted to explore the difference between the transects further (Fig. 3c), but no clear grouping was seen, indicating no obvious difference between transects based on the number and type of polymers.

The mass composition of MPs is addressed in Fig. 3b and d. The composition with respect to mass and counts differed considerably. Take S0809 as an example: ‘others’ dominated by counts, while PE dominated by mass. The PCA analysis shows that S0102 was an outlier compared with the rest of the transects. The separation was mainly determined by ‘others’ (−0.58), PA (−0.55) and polyester (0.52). This can be explained by ‘others’ dominating in S0102. Details on the PCA analysis are discussed in SI.

3.4. Size, shape, and weathering distribution of MPs in marine water

The major and minor dimensions of detected MP and their distribution is shown in Fig. 4a. The minor dimension was calculated as the second dimension of the particle's equivalent ellipse (Simon et al., 2018). A total of 54 % of the MPs could be defined as fragments (major to minor dimensions <3), while the rest were fibers. In terms of mass, the fragments accounted for the same as the number fraction (54 %), while the fibers accounted for the rest (Fig. 4b). The mean and median of all major dimensions were 140 and 86 μm, respectively, while those of the minor dimension were 34 and 26 μm, respectively. Small MPs <100 μm hence dominated the samples (Fig. 4c and d) with 57 % of all MPs being less than this size. In terms of mass, the small fraction constituted 4 % of the total MP mass in the studied waters.

The size distribution per transect is shown in Fig. 4c and d (as well as Fig. S2a and b), illustrating that sizes varied significantly between transects. The largest sizes were found in S1011 while the smallest were found in the neighboring transect S1213. The smallest size range was observed in S1313, with all MPs being <200 μm (Fig. 4c). The most extensive major dimension range was seen in S1213, covering the size range 10–800 μm. The occurrence of large particles in this transect led to a higher mass estimate at moderate counts (Fig. 2).

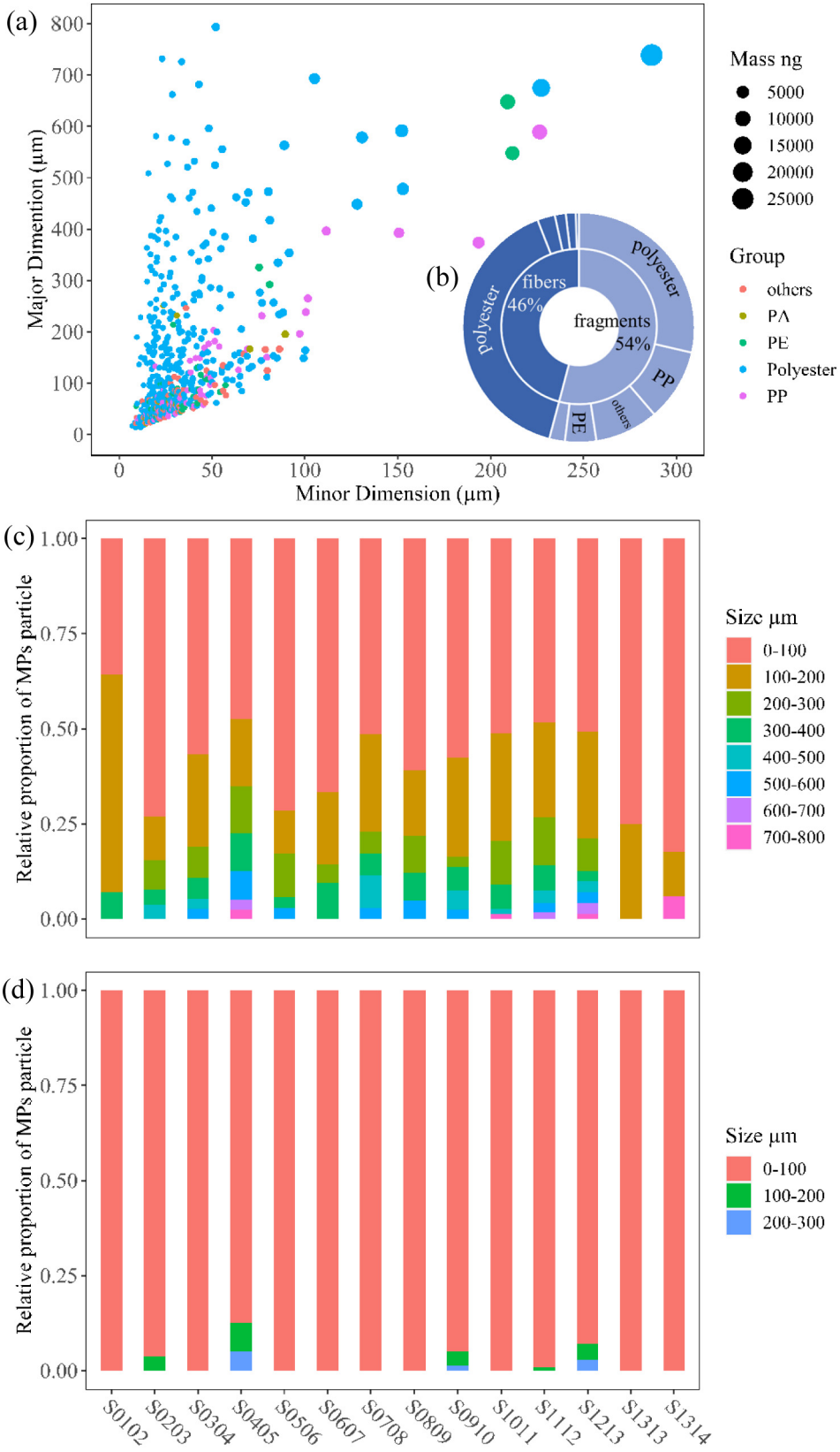

Fig. 4. (a) Bubble plot of minor vs major dimension of all detected MPs in the marine waters. (b) Percentage of MP fibers and fragments for the total analyzed samples. Proportion of size classes per transect of MP based on (c) major dimension and (d) minor dimension.

The carbonyl index of PE and PP differed between transects (Fig. 5a). PP in S1112 showed a much higher carbonyl index than in other transects. However, the uncertainty of this assessment is large as few MPs of these materials were identified in some samples, while others held more (Fig. 5a). Pooling the data and looking at the carbonyl index versus particle size indicated that smaller particles tended to be more oxidized than larger ones (Fig. 5b).

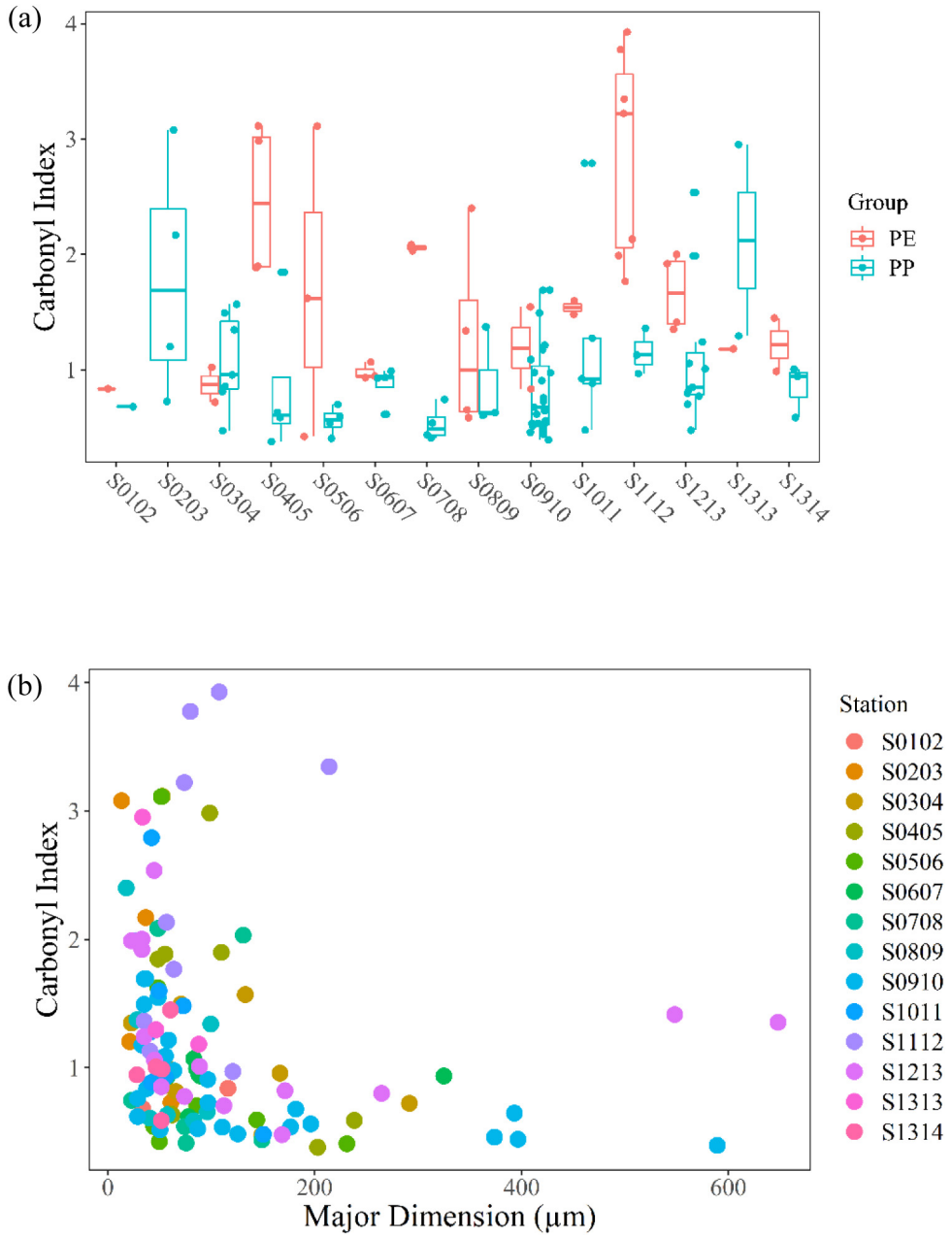

Fig. 5. (a) Boxplot of carbonyl index of the olefins PE and PP at the different stations. The dots show the carbonyl index of individual MPs. The line inside a box shows the median, the button of the box shows the lower quartile, the top its upper quartile. The lower whisker indicates the 5th percentile, while the upper whisker indicates the 95th percentile; (b) Correlation between carbonyl index and Major dimensions of MPs.

4. Discussion

4.1. MP pollution in Kattegat

The concentration of MPs down to 10 μm in the Kattegat and bordering waters ranged from 17 to 286 items m^{-3}, with an average of 103 ± 86 items m^{-3}. These numbers are much higher than what Schönlau et al. (2020) found, namely 2.59 items m^{-3} in Skagerrak and 14.32 items m^{-3} in Kattegat. This difference is probably due to different sampling techniques and analytical methods. Schönlau et al. (2020) used steel filters with mesh sizes of 500, 300 and 50 μm for sampling, while stereomicroscopy and near-infrared hyperspectral imaging of manual selected particles was used to identify MPs and fibers. Smaller particles down to 10 μm were addressed in our study, so it is reasonable that more particles were found, in accordance with other studies that found an inverse relationship between size and number (Zheng et al., 2021). Moreover, the identification of MPs was conducted by imaging with an FPA detector and automated analysis of the acquired image, which is likely to perform better in analyzing MPs, especially the smaller ones, as the automatization reduces human bias. Interestingly, the concentrations in the Kattegat were quite like those reported by Rist et al. (2020) for waters outside Nuuk, Greenland, where 67–278 items m^{-3} were found with a median of 142 items m^{-3}. Rist et al. (2020) employed similar sampling gear and filter sizes, and the sample preparation and MP detection were similar. The mass concentration of MPs ranged from 0.6 to 84.1 μg m^{-3} with an average of 23.3 ± 28.3 μg m^{-3}, also corresponding to what Rist et al. (2020) found for Greenland waters. In terms of mass concentration, MPs in the studied waters were present at similar concentrations as many organic micropollutants, e.g., pharmaceuticals and biocides, typically found in such waters (Bollmann et al., 2019).

It is evident that MP counts and mass show different patterns as few large MPs can contribute much mass but few counts, and vice versa that many small MPs can contribute many counts but little mass (Fig. 2), and there is no simple relation between them (Fig. S2c). The highest counts were found in S1112, while this transect had a mass concentration of 25.1 μg m^{-3}, which is close to the mean of all transects. This illustrates that MP counts do not give the full picture of MPs in a waterbody, and neither does MP mass. Depending on the goal of the study, one or the other, or preferable both, should be stated when reporting MP concentrations (Simon et al., 2018). The observation that there is no simple correlation between MP counts and mass was also highlighted by other researchers, for example Pakhomova et al. (2022), who found moderate MP counts in the Siberian Arctic (0.71 items m^{-3}), which corresponded to their lowest mass concentration (0.6 μg m^{-3}).

4.2. Polymer composition, shape, and size distribution

Polyester dominated in Kattegat and bordering waters, followed by PP and PE. It seems, on the other hand, improbable that polyester should dominate in surface water as it has a density significantly above that of seawater (1.38 g cm^{-3}, Table S1). However, other processes may lead to them staying in the water column, for example, mixing caused by wind where upwards velocities easily can exceed sinking rates (Wang et al., 2020a, 2020b). Other MP shapes would furthermore have even lower sinking rates, and association with lighter-than-water materials, e.g., biofilms, as well as particle agglomeration, might furthermore change the overall density and sinking velocity.

Moreover, polyester is the most common polymer produced for the global market of synthetic fibers, accounting for over 50 % of fiber production (Carr, 2017; Lima et al., 2021). Therefore, it is reasonable that it also was the most common polymer type in our study. Findings on which polymers dominate in marine waters vary, where some studies found polyester to dominate (e.g., Jiang et al., 2020a, 2020b; Lima et al., 2021) while others found other polymers to dominate (e.g. Enders et al., 2015). In wastewater and in discharge from wastewater treatment plants, PP, PE, and polyester often dominate (Horton et al., 2021; F. Liu et al., 2020; Rasmussen et al., 2021; Roscher et al., 2022).

There is, on the other hand, no obvious reason why global or European plastic use should be proportionally reflected in the marine waters of Kattegat as the pathways of discharged plastic might differ. Another thing worth addressing is that the analytical threshold for detecting PE was set a bit conservative to avoid false positives when running siMPle. Partly to avoid other MPs such as PP to be identified as PE, due to the scarcity of peaks in the recorded wave number region of PE spectra, and partly to avoid false PE as described previously and illustrated in Fig. S1. As a result, the PE concentration probably is somewhat underestimated in this study.

As for the shape, fragments (54 %) dominated in our study, which corresponds to what Rist et al. found. It seems reasonable to find more fragments when analyzing for small MP sizes because small fragments can come from breakdown of larger ones as well as breakdown of fibers (Li et al., 2021). Fibers, on the other hand, have been reported to be the most common MP shape when sampling for larger MPs (Zhang et al., 2022). This highlights the difference between sampling with a finer mesh size, which often is done using pumps like in our study, versus sampling with a coarser mesh size, which often is done using small trawl nets. The analytical size quantification limit also matters in this context, as different analytical methods have different lower size limits.

Based on the previous discussion, the size distribution plays a crucial role in explaining the link between number and mass. In this study, relatively large MPs were observed in S0405, S1011 and S1213. This might be a result of the ocean currents in the area. Research has shown that the anticyclonic circulation in the upper layer plays a prominent and persistent role in the Kattegat (Nielsen, 2005). The anticyclonic circulation covers the area from stations 1–4 and 6–9. MPs in these areas might have longer retention time and hence break down more. In the marine environment, the smaller the size, the higher the probability that marine organisms will ingest these MPs, which will increase the potential risk it poses to the ecosystem (Margolis and Bushman, 2014). In this regard, the dominant size of the MPs detected in this study (< 100 μm) overlaps with the prey's size of most common plankton feeding marine organisms (7–150 μm) (Hansen et al., 1994) posing a potential risk to marine organisms. On the other hand, the generally low concentrations detected in this study are likely to represent a minor impact to the pelagic food web (Rist et al., 2020).

4.3. Aging of MPs

The carbonyl index of olefins can in principle give information on the how close a sampling point is to a source as weathering in principle is time dependent when assuming a constant environment. If this holds true, the transects with larger-sized and less weathered MPs should be closer to their sources. In other words, S0102, S0506, S0708, S0809 and S0910 should be closer to their MP source. The map (Fig. 1) shows that these transects are close to the terrestrial environment, but not necessarily to densely inhabited areas. Furthermore, S1112 had a higher carbonyl index than S1213, which is counter to the argument that a longer travel time from the source leads to higher carbonyl index. In general, there was no clear trend that the carbonyl index could be used as suggested above. Why this was the case can only be speculated on. What seems the most robust information to be obtained from the aging of the MPs is that smaller MPs tended to be more oxidized than larger ones. The reason is likely that weathering causes larger items to fragment more readily, leaving the fingerprint of oxidation more pronounced in the small particles. Hence it might mainly give information on the fate processes and less so on the closeness to their source.

4.4. Spatial distribution of MPs

The abundance of MPs showed spatial differences, as displayed in Fig. 2a: the number concentrations (counts) between stations 1 and 9 were substantially lower than those between stations 9 and 12. A possible explanation can be that the storm- and wastewater discharge from the land bordering transects 1–9 is much lower than it is from the densely populated Øresund region, including Copenhagen and Malmö (Fig. S3), which border transects 9–12.

Assuming somewhat simplistically that an inhabitant discharges the same amount of MP to the marine environment irrespectively of where that person lives yields that ‘Hovedstaden’ (station 9 to 12) (Fig. S3) will discharge 10 times more than Nordjylland (station 1 to 3), and 7 times more than ‘Midtjylland’ (station 3 to 5) and ‘Sjælland’ (station 6 to 9). In addition, the Swedish side also contributes significantly by its roughly 1.4 million inhabitants. In comparison, our study indicated that MP abundance in waters bordering ‘Hovedstaden’ was 7 times that of ‘Nordjylland’, and 4 times that of ‘Midtjylland’ and ‘Sjælland’. While this is not a perfect agreement, it indicates that the population centers affected the level of MP pollution of the studied marine environment.

4.5. Potential origins of MPs

One pathway for MPs to reach the marine environment is by urban wastewater and stormwater discharges. Danish and Swedish urban water management is quite similar, and it is reasonable to assume similar wastewater effluent MP content and volume per capita for all land areas bordering Kattegat. The Danish wastewater production in 2019 was 720 million m^3 (Frank-Gopolos et al., 2021), of which ‘Hovedstaden’ (Fig. S3) accounted for roughly 225 million m^3. On top of this comes the Sweden with its around 1.4 million inhabitants, contributing roughly 164 million m^3 per year, which adds up to an annual discharge of treated wastewater of 389 million m^3 to the waters bordering transects 9–12. Assuming an MP concentration in treated effluent of 2390 μg m^{-3} (Rasmussen et al., 2021), leads to an annual discharge of 0.93 tons of MPs. On top of this comes discharges via combined sewer overflows, MPs discharged via separate stormwater, and MPs discharged via sewage illicitly connected to

storm drains. While the amount discharged during storm events is not well known, the phenomenon can be illustrated by the findings of Hitchcock (2020) who sampled at high frequency before, during, and after a heavy storm event that caused flooding in the Cooks River estuary, Australia. He showed that MP abundance increased from 400 particles m^{-3} before the event to up to 17,383 particles m^{-3} after the event (Hitchcock, 2020). No data exist on the MP content of combined sewer overflow, while the total overflow volumes are known at least for Denmark, namely 34 million m^3 in 2019 (Frank-Gopolos et al., 2021). While this is only 5 % in addition to the treated wastewater, the MP content is likely to be substantially higher. The MP content of urban stormwater discharges is also poorly known. For stormwater treated in retention ponds, Liu et al. (2019a, 2019b) found on average 231 μg m^{-3}. However, in Denmark only 56 % of stormwater is treated, and raw stormwater likely holds many times this amount. Finally, storm sewers commonly receive illicitly connected raw wastewater, which estimates have set at 1 %–5 % of all wastewater produced in a well-designed separate sewer system. As raw wastewater contains maybe 50–100 times more MP than treated wastewater (Rasmussen et al., 2021; Simon et al., 2018), this means that this source alone could double the MPs discharged via wastewater.

Another factor contributing to the elevated concentration to the region is the water from the Baltic Sea. The annual average outflow from the Baltic Sea is around 475 km^3 per year, of which about 190 km^3 per year goes via Øresund. According to Kreitsberg et al. (2021) and Uurasjärvi et al. (2021), it contains between 33 and 700 items m^{-3}. Even though these studies used different methods for sampling and analysis, and the results hence are not directly comparable, they still show that the Baltic Sea effluent contributes to the abundance of MPs in the Øresund area.

Apart from the water-borne MPs, the marine environment also receives an unknown number of air-borne MPs (Aves et al., 2022; Bergmann et al., 2019). Their abundance depends on the regional anthropogenic activities, population density, and waste disposal and management practices (Henry et al., 2019). Liu et al. (2019a, 2019b) showed in their study that air-borne MPs with consistent morphology and composition, had high abundance in the atmosphere along the coasts (0.13 ± 0.24 items m^{-3}) as opposed to the pelagic area (0.01 ± 0.01 items m^{-3}), which indicated significant atmospheric transport of MPs to the marine environment (K. Liu et al., 2019b). In other words, the closer to terrestrial systems, the higher the MP concentration.

It is evident that there are many uncertainties and unknowns with respect to the MP load on the Kattegat. In addition, sinks to the sediment compartment are unknown, meaning that not all discharged MPs are represented by the sampled water. Having these many uncertainties in mind, a back-of-the-envelope mass balance can nevertheless be performed: The water of the Øresund area held on average 17.8 μg m^{-3} and the net water flow into Kattegat is 190 km^3 per year. This yields an estimated annual flux into Kattegat of 3.38 tons. The annual MP mass discharged with treated wastewater can be estimated to 0.93 tons. Assuming doubled contribution (discussed before) from stormwater including illicitly connected wastewater and from combined sewer overflows, the contribution from all urban water yields a total mass of 2.79 tons, i.e., around 80 % of the calculated flux into the Kattegat. While the concrete numbers are highly uncertain, this estimate still shows that urban storm- and wastewater discharges are likely to be a non-negligible contribution to MPs in the waters of Kattegat.

4.6. Limitations and perspectives

In this study, the abundance, distribution, composition, and aging of MPs in Danish marine surface water was explored, and the measured concentrations related to population density and associated polluted water discharges. However, MPs are also found in marine sediment, which was not covered in this study. The attempt at a simplified mass balance assumed that the MPs discharged by polluted urban freshwater stay in the water and do not accumulate in the sediment. This is probably only partially correct. It furthermore assumed that MPs in the marine environment are distribute evenly in space and time, which is another assumption not addressed. Finally, the contribution from other sources such as atmospheric deposition was not covered. To establish a solid mass balance, all these and more aspects must be covered, and the knowledge gaps filled.

5. Conclusion

No relationship was identified between MPs measured as number versus mass concentration. Stating the MP concentration of a waterbody by just one of these measures will consequently not give the full picture of how MPs were distributed herein. The most abundant MP polymer type was polyester, followed by PP and PE, with no systematic trend between stations. MPs of sizes <100 μm dominated in both terms of numbers and mass. For the polymer shape, fragments dominated in both number and mass concentration. The aging of polyolefins did not show any systematics with respect to distance to sources. The carbonyl index versus particle size indicated that larger particles (100–300 μm) tended to be less oxidized than smaller ones (10–100 μm) with the smaller particles also showing the highest carbonyl indices. MP levels tended to be the highest close to the large metropolitan center around Øresund. A rough estimate showed that wastewater and stormwater from the region could account for a significant fraction of the MPs in the water entering Kattegat. Consequently, urban water-borne MPs cannot be neglected when assessing the MP content of this waterbody.

CRediT authorship contribution statement

Yuanli Liu: Writing – Original draft preparation, Experimental section, Data Analysis and Visualization; Claudia Lorenz: Supervision, Sampling, Methodology – Spectrum check, Writing- Reviewing and Editing; Alvise Vianello: Supervision, Sampling, Methodology – Library extended, Writing- Reviewing and Editing; Kristian Syberg: Sampling, Writing-Reviewing and Editing; Asbjørn Haaning Nielsen: Sampling, Writing-Reviewing and Editing; Torkel Gissel Nielsen: Sampling, Writing-Reviewing and Editing; Jes Vollertsen: Supervision, Sampling, Funding acquisition; Writing – Reviewing and Editing.

Data availability

Data will be made available on request.

Declaration of competing interest

The authors declare that they have no known competing financial interests or personal relationships that could have appeared to influence the work reported in this paper.

Acknowledgments

This project was funded by the project MarinePlastic (Project no. 25084) for providing financial support to the sampling activities and was furthermore supported by MONPLAS (European Union's Horizon 2020 research and innovation programme under the Marie Skłodowska-Curie grant agreement No 860775. H2020-MSCA-ITN-2019).

Appendix A. Supplementary data

Supplementary data to this article can be found online at https://doi.org/10.1016/j.scitotenv.2022.161255.

References

Akhbarizadeh, R., Dobaradaran, S., Nabipour, I., Tajbakhsh, S., Darabi, A.H., Spitz, J., 2020a. Abundance, composition, and potential intake of microplastics in canned fish. Mar. Pollut. Bull. 160, 111633. https://doi.org/10.1016/J.MARPOLBUL.2020.111633.

Akhbarizadeh, R., Dobaradaran, S., Schmidt, T.C., Nabipour, I., Spitz, J., 2020b. Worldwide bottled water occurrence of emerging contaminants: a review of the recent scientific literature. J. Hazard. Mater. 392, 122271. https://doi.org/10.1016/J.JHAZMAT.2020.122271.

Akhbarizadeh, R., Dobaradaran, S., Amouei Torkmahalleh, M., Saeedi, R., Aibaghi, R., Faraji Ghasemi, F., 2021. Suspended fine particulate matter (PM2.5), microplastics (MPs), and polycyclic aromatic hydrocarbons (PAHs) in air: their possible relationships and health implications. Environ. Res. 192, 110339. https://doi.org/10.1016/J.ENVRES.2020.110339.

Almond, J., Sugumaar, P., Wenzel, M.N., Hill, G., Wallis, C., 2020. Determination of the carbonyl index of polyethylene and polypropylene using specified area under band methodology with ATR-FTIR spectroscopy. E-Polymers 20 (1), 369–381. https://doi.org/10.1515/EPOLY-2020-0041/MACHINEREADABLECITATION/RIS.

Armbruster, D.A., Pry, T., 2008. Limit of blank, limit of detection and limit of quantitation. Clin. Biochem. Rev. 29 (Suppl. 1), S49 /pmc/articles/PMC2556583/.

Aves, A.R., Revell, L.E., Gaw, S., Ruffell, H., Schuddeboom, A., Wotherspoon, N.E., LaRue, M., McDonald, A.J., 2022. First evidence of microplastics in Antarctic snow. Cryosphere 16 (6), 2127–2145. https://doi.org/10.5194/TC-16-2127-2022.

Bagaev, A., Khatmullina, L., Chubarenko, I., 2018. Anthropogenic microlitter in the Baltic Sea water column. Mar. Pollut. Bull. 129 (2), 918–923. https://doi.org/10.1016/J.MARPOLBUL.2017.10.049.

Bakir, A., Desender, M., Wilkinson, T., van Hoytema, N., Amos, R., Airahui, S., Graham, J., Maes, T., 2020. Occurrence and abundance of meso and microplastics in sediment, surface waters, and marine biota from the South Pacific region. Mar. Pollut. Bull. 160, 111572. https://doi.org/10.1016/J.MARPOLBUL.2020.111572.

Beer, S., Garm, A., Huwer, B., Dierking, J., Nielsen, T.G., 2018. No increase in marine microplastic concentration over the last three decades – a case study from the Baltic Sea. Sci. Total Environ. 621, 1272–1279. https://doi.org/10.1016/J.SCITOTENV.2017.10.101.

Bergmann, M., Mützel, S., Primpke, S., Tekman, M.B., Trachsel, J., Gerdts, G., 2019. White and wonderful? Microplastics prevail in snow from the Alps to the Arctic. Sci. Adv. 5 (8). https://doi.org/10.1126/SCIADV.AAX1157/SUPPL_FILE/AAX1157_TABLE_S4.XLSX.

Bollmann, U.E., Simon, M., Vollertsen, J., Bester, K., 2019. Assessment of input of organic micropollutants and microplastics into the Baltic Sea by urban waters. Mar. Pollut. Bull. 148, 149–155. https://doi.org/10.1016/J.MARPOLBUL.2019.07.014.

Buckingham, J.W., Manno, C., Waluda, C.M., Waller, C.L., 2022. A record of microplastic in the marine nearshore waters of South Georgia. Environ. Pollut. 306, 119379. https://doi.org/10.1016/J.ENVPOL.2022.119379.

Carr, S.A., 2017. Invited commentary sources and dispersive modes of micro-fibers in the environment. Integr. Environ. Assess. Manag. 13, 466–469. https://doi.org/10.1002/ieam.1916.

Cole, M., 2016. A novel method for preparing microplastic fibers. Sci. Rep. 6 (1), 1–7. https://doi.org/10.1038/srep34519 2016 6:1.

Cunha, C., Lopes, J., Paulo, J., Faria, M., Kaufmann, M., Nogueira, N., Ferreira, A., Cordeiro, N., 2020. The effect of microplastics pollution in microalgal biomass production: a biochemical study. Water Res. 186, 116370. https://doi.org/10.1016/J.WATRES.2020.116370.

Dai, Z., Zhang, H., Zhou, Q., Tian, Y., Chen, T., Tu, C., Fu, C., Luo, Y., 2018. Occurrence of microplastics in the water column and sediment in an inland sea affected by intensive anthropogenic activities. Environ. Pollut. 242, 1557–1565. https://doi.org/10.1016/J.ENVPOL.2018.07.131.

Duan, J., Bolan, N., Li, Y., Ding, S., Atugoda, T., Vithanage, M., Sarkar, B., Tsang, D.C.W., Kirkham, M.B., 2021. Weathering of microplastics and interaction with other coexisting constituents in terrestrial and aquatic environments. Water Res. 196, 117011. https://doi.org/10.1016/J.WATRES.2021.117011.

Enders, K., Lenz, R., Stedmon, C.A., Nielsen, T.G., 2015. Abundance, size and polymer composition of marine microplastics ≥ 10 μm in the Atlantic Ocean and their modelled vertical distribution. Mar. Pollut. Bull. 100 (1), 70–81. https://doi.org/10.1016/J.MARPOLBUL.2015.09.027.

Eo, S., Hong, S.H., Song, Y.K., Han, G.M., Shim, W.J., 2019. Spatiotemporal distribution and annual load of microplastics in the Nakdong River, South Korea. Water Res. 160, 228–237. https://doi.org/10.1016/J.WATRES.2019.05.053.

Estahbanati, S., Fahrenfeld, N.L., 2016. Influence of wastewater treatment plant discharges on microplastic concentrations in surface water. Chemosphere 162, 277–284. https://doi.org/10.1016/J.CHEMOSPHERE.2016.07.083.

Everaert, G., de Rijcke, M., Lonneville, B., Janssen, C.R., Backhaus, T., Mees, J., van Sebille, E., Koelmans, A.A., Catarino, A.I., Vandegehuchte, M.B., 2020. Risks of floating microplastic in the global ocean. Environ. Pollut. 267, 115499. https://doi.org/10.1016/J.ENVPOL.2020.115499.

Fendall, L.S., Sewell, M.A., 2009. Contributing to marine pollution by washing your face: microplastics in facial cleansers. Mar. Pollut. Bull. 58 (8), 1225–1228. https://doi.org/10.1016/J.MARPOLBUL.2009.04.025.

Ferreira, M., Thompson, J., Paris, A., Rohindra, D., Rico, C., 2020. Presence of microplastics in water, sediments and fish species in an urban coastal environment of Fiji, a Pacific small island developing state. Mar. Pollut. Bull. 153, 110991. https://doi.org/10.1016/J.MARPOLBUL.2020.110991.

Frank-Gopolos, T., Nielsen, L., Skovmark, B., 2021. Punktkilder 2020 (Issue December).

Frias, J.P.G.L., Nash, R., 2019. Microplastics: finding a consensus on the definition. Mar. Pollut. Bull. 138, 145–147. https://doi.org/10.1016/J.MARPOLBUL.2018.11.022.

Gewert, B., Ogonowski, M., Barth, A., MacLeod, M., 2017. Abundance and composition of near surface microplastics and plastic debris in the Stockholm Archipelago, Baltic Sea. Mar. Pollut. Bull. 120 (1–2), 292–302. https://doi.org/10.1016/J.MARPOLBUL.2017.04.062.

Geyer, R., Jambeck, J.R., Law, K.L., 2017. Production, use, and fate of all plastics ever made. Sci. Adv. 3 (7). https://doi.org/10.1126/SCIADV.1700782/SUPPL_FILE/1700782_SM.PDF.

Gröger, M., Arneborg, L., Dieterich, C., Höglund, A., Meier, H.E.M., 2019. Summer hydrographic changes in the Baltic Sea, Kattegat and Skagerrak projected in an ensemble of climate scenarios downscaled with a coupled regional ocean–sea ice–atmosphere model. Clim. Dyn. 53 (9–10), 5945–5966. https://doi.org/10.1007/S00382-019-04908-9/FIGURES/12.

Hansen, B., Bjornsen, P.K., Hansen, P.J., 1994. The size ratio between planktonic predators and their prey. Limnol. Oceanogr. 39 (2), 395–403. https://doi.org/10.4319/LO.1994.39.2.0395.

Henry, B., Laitala, K., Klepp, I.G., 2019. Microfibres from apparel and home textiles: prospects for including microplastics in environmental sustainability assessment. Sci. Total Environ. 652, 483–494. https://doi.org/10.1016/J.SCITOTENV.2018.10.166.

Hitchcock, J.N., 2020. Storm events as key moments of microplastic contamination in aquatic ecosystems. Sci. Total Environ. 734, 139436. https://doi.org/10.1016/J.SCITOTENV.2020.139436.

Horton, A.A., Cross, R.K., Read, D.S., Jürgens, M.D., Ball, H.L., Svendsen, C., Vollertsen, J., Johnson, A.C., 2021. Semi-automated analysis of microplastics in complex wastewater samples. Environ. Pollut. 268, 115841. https://doi.org/10.1016/J.ENVPOL.2020.115841.

Jaikumar, G., Brun, N.R., Vijver, M.G., Bosker, T., 2019. Reproductive toxicity of primary and secondary microplastics to three cladocerans during chronic exposure. Environ. Pollut. 249, 638–646. https://doi.org/10.1016/J.ENVPOL.2019.03.085.

Jiang, Y., Yang, F., Zhao, Y., Wang, J., 2020. Greenland Sea gyre increases microplastic pollution in the surface waters of the nordic seas. Sci. Total Environ. 712, 136484. https://doi.org/10.1016/J.SCITOTENV.2019.136484.

Jiang, Y., Zhao, Y., Wang, X., Yang, F., Chen, M., Wang, J., 2020. Characterization of microplastics in the surface seawater of the South Yellow Sea as affected by season. Sci. Total Environ. 724, 138375. https://doi.org/10.1016/J.SCITOTENV.2020.138375.

Kashfi, F.S., Ramavandi, B., Arfaeinia, H., Mohammadi, A., Saeedi, R., De-la-Torre, G.E., Dobaradaran, S., 2022. Occurrence and exposure assessment of microplastics in indoor dusts of buildings with different applications in Bushehr and Shiraz cities, Iran. Sci. Total Environ. 829, 154651. https://doi.org/10.1016/J.SCITOTENV.2022.154651.

Kreitsberg, Randel, Raudna-Kristoffersen, Merilin, Heinlaan, Margit, Ward, Raymond, Visnapuu, Meeri, Kisand, Vambola, Meitern, Richard, Kotta, Jonne, Tuvikene, Arvo, 2021. Seagrass beds reveal high abundance of microplastic in sediments: A case study in the Baltic Sea. Mar. Pollut. Bull. (ISSN: 0025-326X) 168, 112417. https://doi.org/10.1016/j.marpolbul.2021.112417.

Li, W.C., Tse, H.F., Fok, L., 2016. Plastic waste in the marine environment: a review of sources, occurrence and effects. Sci. Total Environ. 566–567, 333–349. https://doi.org/10.1016/J.SCITOTENV.2016.05.084.

Li, C., Wang, X., Liu, K., Zhu, L., Wei, N., Zong, C., Li, D., 2021. Pelagic microplastics in surface water of the eastern Indian Ocean during monsoon transition period: abundance, distribution, and characteristics. Sci. Total Environ. 755, 142629. https://doi.org/10.1016/J.SCITOTENV.2020.142629.

Lima, A.R.A., Ferreira, G.V.B., Barrows, A.P.W., Christiansen, K.S., Treinish, G., Toshack, M.C., 2021. Global patterns for the spatial distribution of floating microfibers: Arctic Ocean as a potential accumulation zone. J. Hazard. Mater. 403, 123796. https://doi.org/10.1016/J.JHAZMAT.2020.123796.

Lindeque, P.K., Cole, M., Coppock, R.L., Lewis, C.N., Miller, R.Z., Watts, A.J.R., Wilson-McNeal, A., Wright, S.L., Galloway, T.S., 2020. Are we underestimating microplastic abundance in the marine environment? A comparison of microplastic capture with nets of different mesh-size. Environ. Pollut. 265, 114721. https://doi.org/10.1016/J.ENVPOL.2020.114721.

Liu, F., Olesen, K.B., Borregaard, A.R., Vollertsen, J., 2019. Microplastics in urban and highway stormwater retention ponds. Sci. Total Environ. 671, 992–1000. https://doi.org/10.1016/J.SCITOTENV.2019.03.416.

Liu, K., Wu, T., Wang, X., Song, Z., Zong, C., Wei, N., Li, D., 2019. Consistent transport of terrestrial microplastics to the ocean through atmosphere. Environ. Sci. Technol. 53 (18), 10612–10619. https://doi.org/10.1021/ACS.EST.9B03427/SUPPL_FILE/ES9B03427_SI_002.PDF.

Liu, F., Nord, N.B., Bester, K., Vollertsen, J., 2020. Microplastics removal from treated wastewater by a biofilter. Water 12 (4), 1085. https://doi.org/10.3390/W12041085 2020, Vol. 12, Page 1085.

Liu, M., Ding, Y., Huang, P., Zheng, H., Wang, W., Ke, H., Chen, F., Liu, L., Cai, M., 2021. Microplastics in the western Pacific and South China Sea: spatial variations reveal the impact of kuroshio intrusion. Environ. Pollut. 288, 117745. https://doi.org/10.1016/J.ENVPOL.2021.117745.

Löder, M.G.J., Imhof, H.K., Ladehoff, M., Löschel, L.A., Lorenz, C., Mintenig, S., Piehl, S., Primpke, S., Schrank, I., Laforsch, C., Gerdts, G., 2017. Enzymatic purification of microplastics in environmental samples. Environ. Sci. Technol. 51 (24), 14283–14292. https://doi.org/10.1021/ACS.EST.7B03055/SUPPL_FILE/ES7B03055_SI_001.PDF.

Lorenz, C., Roscher, L., Meyer, M.S., Hildebrandt, L., Prume, J., Löder, M.G.J., Primpke, S., Gerdts, G., 2019. Spatial distribution of microplastics in sediments and surface waters of the southern North Sea. Environ. Pollut. 252, 1719–1729. https://doi.org/10.1016/J.ENVPOL.2019.06.093.

Mahon, A.M., O'Connell, B., Healy, M.G., O'Connor, I., Officer, R., Nash, R., Morrison, L., 2017. Microplastics in sewage sludge: effects of treatment. Environ. Sci. Technol. 51 (2), 810–818. https://doi.org/10.1021/ACS.EST.6B04048/SUPPL_FILE/ES6B04048_SI_001.PDF.

Mani, T., Primpke, S., Lorenz, C., Gerdts, G., Burkhardt-Holm, P., 2019. Microplastic Pollution in Benthic Midstream Sediments of the Rhine River. https://doi.org/10.1021/acs.est.9b01363.

Margolis, D., Bushman, F., 2014. Persistence by proliferation? Science 345 (6193), 143–144. https://doi.org/10.1126/SCIENCE.1257426/ASSET/A01678D8-AA58-4EDA-81DF-0385530B18B1/ASSETS/GRAPHIC/345_143_F1.JPEG.

Mathalon, A., Hill, P., 2014. Microplastic fibers in the intertidal ecosystem surrounding Halifax Harbor, Nova Scotia. Mar. Pollut. Bull. 81 (1), 69–79. https://doi.org/10.1016/J.MARPOLBUL.2014.02.018.

Mei, W., Chen, G., Bao, J., Song, M., Li, Y., Luo, C., 2020. Interactions between microplastics and organic compounds in aquatic environments: a mini review. Sci. Total Environ. 736, 139472. https://doi.org/10.1016/J.SCITOTENV.2020.139472.

Mu, J., Zhang, S., Qu, L., Jin, F., Fang, C., Ma, X., Zhang, W., Wang, J., 2019. Microplastics abundance and characteristics in surface waters from the Northwest Pacific, the Bering Sea, and the Chukchi Sea. Mar. Pollut. Bull. 143, 58–65. https://doi.org/10.1016/J.MARPOLBUL.2019.04.023.

Nielsen, M.H., 2005. The baroclinic surface currents in the Kattegat. J. Mar. Syst. 55 (3–4), 97–121. https://doi.org/10.1016/J.JMARSYS.2004.08.004.

Pakhomova, Svetlana, Berezina, Anfisa, Lusher, Amy L., Zhdanov, Igor, Silvestrova, Ksenia, Zavialov, Peter, van Bavel, Bert, Yakushev, Evgeniy, 2022. Microplastic variability in subsurface water from the Arctic to Antarctica. Environ. Pollut. (ISSN: 0269-7491) 298, 118808. https://doi.org/10.1016/j.envpol.2022.118808.

Pan, Z., Guo, H., Chen, H., Wang, S., Sun, X., Zou, Q., Zhang, Y., Lin, H., Cai, S., Huang, J., 2019. Microplastics in the northwestern Pacific: abundance, distribution, and characteristics. Sci. Total Environ. 650, 1913–1922. https://doi.org/10.1016/J.SCITOTENV.2018.09.244.

Pan, Z., Liu, Q., Sun, Y., Sun, X., Lin, H., 2019. Environmental implications of microplastic pollution in the northwestern Pacific Ocean. Mar. Pollut. Bull. 146, 215–224. https://doi.org/10.1016/J.MARPOLBUL.2019.06.031.

Physical Oceanography of the Baltic Sea, .. Matti Leppäranta, Kai Myrberg - Google Books https://books.google.de/books?id=csLKtvZNV98C&pg=PA74&redir_esc=y#v=onepage&q&f=false 2016 6:1.

Primpke, S., Wirth, M., Lorenz, C., Gerdts, G., 2018. Reference database design for the automated analysis of microplastic samples based on fourier transform infrared (FTIR) spectroscopy. Anal. Bioanal. Chem. 410, 5131–5141. https://doi.org/10.1007/s00216-018-1156-x.

Primpke, S., Cross, R.K., Mintenig, S.M., Simon, M., Vianello, A., Gerdts, G., Vollertsen, J., 2020. Toward the systematic identification of microplastics in the environment: evaluation of a new independent software tool (siMPle) for spectroscopic analysis. Appl. Spectrosc. 74 (9), 1127–1138. https://doi.org/10.1177/0003702820917760.

Rasmussen, L.A., Iordachescu, L., Tumlin, S., Vollertsen, J., 2021. A complete mass balance for plastics in a wastewater treatment plant - macroplastics contributes more than microplastics. Water Res. 201, 117307. https://doi.org/10.1016/J.WATRES.2021.117307.

Renner, G., Schmidt, T.C., Schram, J., 2018. Analytical methodologies for monitoring micro (nano)plastics: which are fit for purpose? Curr. Opin. Environ. Sci. Health 1, 55–61. https://doi.org/10.1016/J.COESH.2017.11.001.

Rist, S., Vianello, A., Winding, M.H.S., Nielsen, T.G., Almeda, R., Torres, R.R., Vollertsen, J., 2020. Quantification of plankton-sized microplastics in a productive coastal Arctic marine ecosystem. Environ. Pollut. 266, 115248. https://doi.org/10.1016/J.ENVPOL.2020.115248.

Roscher, L., Halbach, M., Nguyen, M.T., Hebeler, M., Luschtinetz, F., Scholz-Böttcher, B.M., Primpke, S., Gerdts, G., 2022. Microplastics in two german wastewater treatment plants: year-long effluent analysis with FTIR and py-GC/MS. Sci. Total Environ. 817, 152619. https://doi.org/10.1016/J.SCITOTENV.2021.152619.

Schönlau, C., Karlsson, T.M., Rotander, A., Nilsson, H., Engwall, M., van Bavel, B., Kärrman, A., 2020. Microplastics in sea-surface waters surrounding Sweden sampled by manta trawl and in-situ pump. Mar. Pollut. Bull. 153, 111019. https://doi.org/10.1016/J.MARPOLBUL.2020.111019.

Setälä, O., Magnusson, K., Lehtiniemi, M., Norén, F., 2016. Distribution and abundance of surface water microlitter in the Baltic Sea: a comparison of two sampling methods. Mar. Pollut. Bull. 110 (1), 177–183. https://doi.org/10.1016/J.MARPOLBUL.2016.06.065.

Simon, M., van Alst, N., Vollertsen, J., 2018. Quantification of microplastic mass and removal rates at wastewater treatment plants applying focal plane Array (FPA)-based fourier transform infrared (FT-IR) imaging. Water Res. 142, 1–9. https://doi.org/10.1016/J.WATRES.2018.05.019.

Simon-Sánchez, L., Grelaud, M., Franci, M., Ziveri, P., 2022a. Are research methods shaping our understanding of microplastic pollution? A literature review on the seawater and sediment bodies of the Mediterranean Sea. Environ. Pollut. 292, 118275. https://doi.org/10.1016/J.ENVPOL.2021.118275.

Simon-Sánchez, L., Grelaud, M., Lorenz, C., Garcia-Orellana, J., Vianello, A., Liu, F., Vollertsen, J., Ziveri, P., 2022b. Can a sediment core reveal the plastic age? Microplastic preservation in a coastal sedimentary record. Environ. Sci. Technol. https://doi.org/10.1021/ACS.EST.2C04264.

Sridhar, A., Kannan, D., Kapoor, A., Prabhakar, S., 2022. Extraction and detection methods of microplastics in food and marine systems: a critical review. Chemosphere 286, 131653. https://doi.org/10.1016/J.CHEMOSPHERE.2021.131653.

Sundt, P., Schulze, P.E., Syversen, F., 2014. Sources of microplastic-pollution to the marine environment. Report no. M-321|2015. Norwegian Environment Agency. https://www.miljodirektoratet.no/globalassets/publikasjoner/M321/M321.pdf.

Syberg, K., Knudsen, C.M.H., Tairova, Z., Khan, F., Shashoua, Y., Geertz, T., Pedersen, H.B., Sick, C., Knudsen, T.B., Jørgensen, J.H., Palmqvist, A., 2017. Abundance of Microplastics and Adhered Contaminants in the North Atlantic Ocean. Fate and Impact of Microplastics in Marine Ecosystems, p. 158 https://doi.org/10.1016/B978-0-12-812271-6.00159-9.

Tamminga, M., Hengstmann, E., Fischer, E.K., 2018. Microplastic analysis in the south funen archipelago, Baltic Sea, implementing manta trawling and bulk sampling. Mar. Pollut. Bull. 128, 601–608. https://doi.org/10.1016/J.MARPOLBUL.2018.01.066.

Teng, J., Zhao, J., Zhang, C., Cheng, B., Koelmans, A.A., Wu, D., Gao, M., Sun, X., Liu, Y., Wang, Q., 2020. A systems analysis of microplastic pollution in Laizhou Bay, China. Sci. Total Environ. 745, 140815. https://doi.org/10.1016/J.SCITOTENV.2020.140815.

Turgay, E., Steinum, T.M., Colquhoun, D., Karataş, S., 2019. Environmental biofilm communities associated with early-stage common dentex (Dentex dentex) culture. J. Appl. Microbiol. 126 (4), 1032–1043. https://doi.org/10.1111/JAM.14205.

Uurasjärvi, Emilia, Pääkkönen, Minna, Setälä, Outi, Koistinen, Arto, Lehtiniemi, Maiju, 2021. Microplastics accumulate to thin layers in the stratified Baltic Sea. Environ. Pollut. (ISSN: 0269-7491) 268, 115700. https://doi.org/10.1016/j.envpol.2020.115700 Part A.

Vianello, A., Jensen, R.L., Liu, L., Vollertsen, J., 2019. Simulating human exposure to indoor airborne microplastics using a Breathing Thermal Manikin. Sci. Rep. 9 (1), 1–11. https://doi.org/10.1038/s41598-019-45054-w 2019 9:1.

Wang, C., Xian, Z., Jin, X., Liang, S., Chen, Z., Pan, B., Wu, B., Ok, Y.S., Gu, C., 2020. Photoaging of polyvinyl chloride microplastic in the presence of natural organic acids. Water Res. 183, 116082. https://doi.org/10.1016/J.WATRES.2020.116082.

Wang, H., Dong, C., Yang, Y., Gao, X., 2020. Parameterization of wave-induced mixing using the large eddy simulation (LES) (I). Atmosphere 11 (2), 207. https://doi.org/10.3390/ATMOS11020207 2020, Vol. 11, Page 207.

Wright, S.L., Thompson, R.C., Galloway, T.S., 2013. The physical impacts of microplastics on marine organisms: a review. Environ. Pollut. 178, 483–492. https://doi.org/10.1016/J.ENVPOL.2013.02.031.

Ye, Y., Yu, K., Zhao, Y., 2022. The development and application of advanced analytical methods in microplastics contamination detection: a critical review. Sci. Total Environ. 818, 151851. https://doi.org/10.1016/J.SCITOTENV.2021.151851.

Zhang, W., Zhang, S., Wang, J., Wang, Y., Mu, J., Wang, P., Lin, X., Ma, D., 2017. Microplastic pollution in the surface waters of the Bohai Sea, China. Environ. Pollut. 231, 541–548. https://doi.org/10.1016/J.ENVPOL.2017.08.058.

Zhang, S., Zhang, W., Ju, M., Qu, L., Chu, X., Huo, C., Wang, J., 2022. Distribution characteristics of microplastics in surface and subsurface Antarctic seawater. Sci. Total Environ. 838, 156051. https://doi.org/10.1016/J.SCITOTENV.2022.156051.

Zhao, S., Zhu, L., Li, D., 2015. Microplastic in three urban estuaries, China. Environ. Pollut. 206, 597–604. https://doi.org/10.1016/J.ENVPOL.2015.08.027.

Zheng, Y., Li, J., Sun, C., Cao, W., Wang, M., Jiang, F., Ju, P., 2021. Comparative study of three sampling methods for microplastics analysis in seawater. Sci. Total Environ. 765, 144495. https://doi.org/10.1016/J.SCITOTENV.2020.144495.

Zhou, Q., Tu, C., Yang, J., Fu, C., Li, Y., Waniek, J.J., 2021. Trapping of microplastics in halocline and turbidity layers of the semi-enclosed Baltic Sea. Front. Mar. Sci. 8, 1555. https://doi.org/10.3389/FMARS.2021.761566/BIBTEX.